A stress-responsive glyoxalase I from the parasitic nematode *Onchocerca volvulus*

Alexandra SOMMER*, Peter FISCHER†, Kristina KRAUSE*, Kay BOETTCHER‡, Peter M. BROPHY§, Rolf D. WALTER* and Eva LIEBAU*[1]

*Department of Biochemistry, Bernhard Nocht Institute for Tropical Medicine, Bernhard-Nocht-Strasse 74, 20359 Hamburg, Germany, †Department of Molecular Biology, Bernhard Nocht Institute for Tropical Medicine, Bernhard-Nocht-Strasse 74, 20359 Hamburg, Germany, ‡LION Bioscience AG, Im Neuenheimer Feld 515–517, 69120 Heidelberg, Germany, and §Institute of Biological Sciences, University of Wales, Aberystwyth, Ceredigon SY23 3DA, U.K.

Glyoxal, methylglyoxal and other physiological α-oxoaldehydes are formed by the lipid peroxidation, glycation and degradation of glycolytic intermediates. They are detoxified enzymically by the glyoxalase system. To investigate the physiological function of glyoxalase I in parasitic organisms, the cDNA for glyoxalase I from the filarial nematode *Onchocerca volvulus* (designated *Ov*-GloI) has been cloned and characterized. The isolated cDNA contains an open reading frame of 579 bp encoding a protein with a calculated molecular mass of 21930 Da. Owing to the high degree of sequence identity (60 %) with human glyoxalase I, for which the X-ray structure is available, it has been possible to build a three-dimensional model of *Ov*-GloI. The modelled core of *Ov*-GloI is conserved compared with the human glyoxalase I; however, there are critical differences in the residues lining the hydrophobic substrate-binding pocket of *Ov*-GloI. A 22 kDa protein was obtained by heterologous expression in *Escherichia coli*. A homogeneous enzyme preparation was obtained by affinity purification and functional characterization of the recombinant enzyme included the determination of kinetic constants for methylglyoxal and phenylglyoxal as well as inhibition studies. Gel filtration demonstrated a dimeric structure. To assess the role of *Ov*-GloI as a potential vaccine candidate or serodiagnostic tool, the serological reactivity of the recombinant *Ov*-GloI was analysed with sera from microfilaria carriers and specific IgG1 antibodies were detected. The effects of oxidative insult, namely plumbagin and xanthine/xanthine oxidase, on the gene transcript level of *Ov*-GloI were investigated. By using a semi-quantitative PCR ELISA it was shown that *Ov*-GloI is expressed at elevated levels under conditions of oxidative stress.

Key words: glutathione, oxidative stress, parasite.

INTRODUCTION

Onchocerca volvulus is the causative agent of onchocerciasis, a disease that affects approx. 18 million people in subsaharan Africa. One of the major pathological consequences of the infection is ocular damage (river blindness) caused by larvae (microfilariae) that are released in millions by the adult females (macrofilariae) during their 10–14-year life span. Although ivermectin is effective in killing the microfilariae, there is an urgent need for the development of better and safer drugs that are effective against adult worms [1].

The glyoxalase system is an important but frequently neglected component of glutathione-dependent enzymology. It is a relatively simple pathway consisting of two consecutive enzymic reactions catalysed by glyoxalase I (lactoylglutathione lyase; EC 4.4.1.5) and glyoxalase II (hydroxyacylglutathione hydrolase; EC 3.1.2.6). Glyoxalase I is an isomerase that catalyses the formation of (*S*)-D-lactoylglutathione from the hemimercaptal adduct that forms spontaneously between methylglyoxal and glutathione. The *S*-ester product is then hydrolysed by glyoxalase II into D-lactic acid and glutathione. The physiological substrates of glyoxalase I are glyoxal, formed from lipid peroxidation and glycation reactions; methylglyoxal, formed from triose phosphates, ketone body metabolism and threonine catabolism; and 4,5-dioxovalerate, formed from 5-aminolaevulinate and α-oxoglutarate. The pathway is found in all organisms; glyoxalase phenotypes are among the earliest expressed in embryogenesis and persist throughout development, maturation and senescence. The widespread distribution and presence of this shunt pathway indicates a universal role in primary metabolism. However, the biological function of the pathway remains unclear (reviewed in [2–4]).

Because α-oxoaldehyes are cytostatic at low concentrations and cytotoxic at high concentration, the glyoxalase system is thought to be involved in detoxication. In the cell, α-oxoaldehydes react with guanyl residues of DNA and RNA and this can cause mutagenesis and apoptosis [5]; they also react with cysteine, lysine and arginine residues in proteins and this can lead to protein cross-linking and degradation and the activation of a proinflammatory response of monocytes and macrophages [6].

Reports demonstrate that different stress conditions, such as salt stress in plants, tumour implantation into animals or glycerol load in bacteria, result in an induction of glyoxalases. Similar changes have also been observed in humans under stress due to excercise or in animals after irradiation [7]. The induction is possibly due to the higher demand for glyoxalase caused by the increased rate of glycolysis during stress.

Host immune-dependent damage to parasites can be mediated by several mechanisms including the production of oxygen radicals following the respiratory burst by myeloid cells, the action of myeloperoxidase and eosinophil peroxidase from neutrophils and eosinophils, or via a nitric oxide response that is particularly high in macrophages [8]. The primary consequence of this generation of oxidants lies in the degradation of membrane

Abbreviations used: GST, glutathione S-transferase; IPTG, isopropyl β-D-thiogalactoside; *Ov*-GloI, glyoxalase I from *Onchocerca volvulus*; r*Ov*-GloI, recombinant *Ov*-GloI; RT–PCR, reverse-transcriptase-mediated PCR.

[1] To whom correspondence should be addressed (e-mail liebau@bni.uni-hamburg.de).

The nucleotide sequence data for *Onchocerca volvulus* glyoxalase I reported will appear in DDBJ, EMBL and GenBank Nucleotide Sequence Databases under the accession numbers AI815247 and AA666427.

lipids or, more specifically, their polyunsaturated fatty acyl moieties through the chain reaction of lipid peroxidation. The parasite can respond to this host-induced stress by employing a succession of defences, which we propose also to include, in an adapted manner, the detoxification of α-oxoaldehydes by the action of the glyoxalase system.

The glyoxalase system of parasites has not been investigated with molecular biological methods. Two studies on helminth glyoxalases with somatic extracts demonstrated that parasitic nematodes possess high activities of glyoxalase I and II, whereas glyoxalase II activity could not be measured in trematodes [9,10]. Here we report the cloning and characterization of a glyoxalase I from *O. volvulus*, designated *Ov*-GloI. To assess the role of *Ov*-GloI as potential vaccine candidate or diagnostic antigen, the serological reactivity of recombinant *Ov*-GloI (r*Ov*-GloI) with sera from microfilaria carriers was analysed. In addition, because the induction of *Ov*-GloI might be linked to survival of the parasite, in response to immunological or drug-related stress, we have analysed this response under conditions of oxidative stress.

MATERIALS AND METHODS

Parasites

Onchocercomata were removed by nodulectomy from untreated patients with generalized onchocerciasis in Benin, as described previously [11]. Nodulectomies for research purposes were approved by the Ethics Commission of the Medical Board Hamburg. The worms were isolated from the nodules by microdissection, incubated in RPMI 1640 containing 0.5 % collagenase (*Clostridium histolyticum*; Boehringer Mannheim) and checked microscopically for purity from host material and for viability.

Maintenance *in vitro* and stress induction of adult *O. volvulus*

Viable adult female worms were allowed to recover at 37 °C for 6–12 h in RPMI 1640 supplemented with 100 units/ml penicillin, 100 μg/ml streptomycin and 250 ng/ml fungizone. The effects of reactive oxygen intermediates on mRNA levels of *Ov*-GloI were investigated by applying several biochemical model reactions. The generation of reactive oxygen intermediates ($O_2^{-\bullet}$, H_2O_2 and $OH^{\bullet}$) was initiated by the addition of xanthine and xanthine oxidase. Additional experiments to examine the effects of $O_2^{-\bullet}$ were performed with plumbagin (5-hydroxy-2-methyl-1,4-napthoquinone). Three adult female worms were used for a single individual stress experiment; each experiment was performed twice. The worms were incubated for 2 h under different stress conditions (50 μM plumbagin or 1 mM xanthine/1 m-unit of xanthine oxidase). After incubation, worms were recovered and washed extensively in RPMI 1640 medium, then finally snap-frozen in liquid nitrogen.

Preparation of RNA and first-strand oligo(dT)-primed cDNA synthesis

Worms were crushed under liquid nitrogen with a ceramic mortar and pestle, then resuspended in TRIzol reagent; total RNA was prepared in accordance with the manufacturer's instructions. Total RNA was treated with DNase I and, after extraction with phenol and precipitation with ethanol, first-strand oligo(dT)-primed cDNA synthesis was performed in 20 μl reactions consisting of 0.2 μg of total RNA, 25 mM Tris/HCl, pH 8.3, 38 mM KCl, 1.5 mM $MgCl_2$, 5 mM dithiothreitol, 20 μM dNTP mix and 0.2 μM one-base-anchored oligo(dT) primer. Reaction mixtures were incubated at 65 °C for 5 min and 37 °C for an initial 10 min, after which 100 units of Moloney murine leukemia virus ('MMLV') reverse transcriptase was added. An additional incubation for 60 min was followed by heating of the reactions at 75 °C for 5 min and then cooling to 4 °C.

Isolation of the complete cDNA encoding *Ov*-GloI

In a survey for genes that are overexpressed in *O. volvulus* after chemotherapy with the microfilaricidal drug ivermectin, a unidirectional cDNA library was constructed in the lambda Uni-Zap XR vector. Subsequently, an expressed-sequence-tag analysis of the cDNA library was performed. The library was plated out with XL1-Blue cells (Stratagene) as host. Recombinant clones were picked at random and their inserts were amplified by PCR with T3/T7 primers. The PCR product was purified and sequenced by direct cycle sequencing. A BLAST search analysis of an obtained PCR product demonstrated moderate similarity to glyoxalase I forms from different organisms.

Modelling, model refinement and structure validation

Three-dimensional models were generated on the basis of the crystal structure of human glyoxalase I (Brookhaven Protein Data Bank entry code, Ijro VRML; PDB code, 1BH5) [12]. The initial three-dimensional models were generated by the MODELLER4 package [13]. Modelling of the three-dimensional structure of *Ov*-GloI followed a standard stepwise procedure. The alignment was performed with the MALIGN program. Owing to the missing counterpart of the N-terminal 15 amino acid residues (M1 to A15 in the *Ov*-GloI sequence), this stretch of amino acids was omitted in the modelling steps. After initial modelling, a first energy-minimization step was performed with the CHARMM force field [14]. After superpositioning of the protein structures, the coordinates of the Zn^{2+} ion and the *S*-hexylglutathione molecule were transferred from the human glyoxalase I structure to the *Ov*-GloI model. Further refinements of the complete protein inhibitor complex were performed with the Amber force field [15]. Subsequently, energy minimization was performed with 100 steps of steepest descent followed by 100 steps of a quasi-Newton minimization [16] to alleviate steric clashes between atoms and to obtain a reasonable peptide geometry. The quality of the model was assessed by different validation tools. In each step of model-building, the *Ov*-GloI structure was validated with the program PROCHECK [17]. No significant geometric violations were detected in the final model. The root-mean-square deviations of Cα atoms between human glyoxalase I and *Ov*-GloI were 0.47 and 0.71 Å for the A-chain and B-chain respectively. Molecular visualization was performed with the programs MOLSCRIPT and Raster3D [18].

Northern blot analysis

For identification of the *Ov*-GloI transcript, 30 μg of total RNA was separated on a 1 % (w/v) agarose gel containing 2.2 M formaldehyde, then blotted to a nylon membrane. The membrane was then hybridized with a [^{32}P]dATP-labelled cDNA probe.

Construction of expression plasmids, expression of *Ov*-GloI in *Escherichia coli* and purification of r*Ov*-GloI

To synthesize the *Ov*-GloI coding region for expression in *E. coli*, the sense oligonucleotide 7684 (5′-CCGCTCGAGGGGCTCG-ACTCAGTGCGAATCAGGA-3′), encoding the first eight residues of the *Ov*-GloI cDNA, and the anti-sense oligonucleotide 7686 (5′-CCCCCGGGAGAGTTTTACACATTCAAAAGAT-AATT-3′), encoding the last eight residues of the *Ov*-GloI cDNA, were used in PCR with the complete *Ov*-GloI cDNA as template. The sense primer contained an *Xho*I restriction site and the anti-sense primer a *Sma*I restriction site to simplify directed,

in-frame cloning into pJC40 [19]. The constructs were transformed into *E. coli* BL21 (DE3) and used for the expression of r*Ov*-GloI. Transformed bacterial cells were grown overnight in Luria–Bertani medium containing 50 μg/ml ampicillin and supplemented with 1 mM $ZnSO_4$ and 10 % (v/v) glycerol [18]. This stock culture was diluted 1:100 in the same medium, then the bacteria were grown to a D_{600} of 0.5 before induction with 1 mM isopropyl β-D-thiogalactoside (IPTG). After 3 h at 37 °C, bacterial cells were harvested and r*Ov*-GloI was isolated by resuspension of bacterial cells in 10 mM Tris/HCl, pH 7.8, followed by sonication and centrifugation at 100000 ***g*** (1 h, 4 °C; TFT 55.38 rotor, Centrikon T-1065; Kontron). The r*Ov*-GloI was purified with na *S*-hexylgutathione affinity matrix. Because the protein was eluted with *S*-hexylglutathione, a potential inhibitor of *Ov*-GloI, the purified r*Ov*-GloI was dialysed overnight against 10 mM Tris/HCl (pH 7.8)/0.1 mM dithiothreitol [20].

Assay of glyoxalase I activity and kinetic studies

Specific activity was determined spectrophotometrically as described in [2,21]. In brief, the glyoxalase-catalysed transformation of the glutathione adduct of methylglyoxal was followed spectrophotometrically by the increase in A_{240} (ϵ 2.86 $mM^{-1} \cdot cm^{-1}$). The hemimercaptal was prepared by preincubating 2 mM methylglyoxal and 2 mM glutathione in 0.05 M sodium phosphate buffer, pH 6.6, for 5 min; the reference sample was incubated similarly but omitting *Ov*-GloI. The equilibrium hemithioacetal concentration was 0.63 mM. Steady-state kinetic measurements with phenylglyoxal were made spectrophotometrically at the apparent isosbestic point of 263 nm. The molar absorption coefficient between α-oxoaldehyde and hemimercaptal is 5.69 $mM^{-1} \cdot cm^{-1}$ for phenylglyoxal. The equilibrium constants used for the determination of the hemimercaptal concentration were 0.6 mM for phenylglyoxal and 3.0 mM for methylglyoxal. Kinetic constants were determined in conditions under which the initial rates were proportional to the enzyme concentrations. K_m and the apparent limiting velocity, V_{max}, were determined by the double-reciprocal method of Lineweaver and Burk.

Inhibition studies

IC_{50} values for r*Ov*-GloI were determined at fixed concentrations of methylglyoxal and glutathione at an adduct concentration of 20 μM. The concentration of free glutathione was kept at 0.1 mM [20,21].

Gel-filtration chromatography

FPLC was performed on a High Load Superdex 75 column (16 cm × 1.6 cm; Pharmacia) that had been equilibrated with 50 mM Tris/HCl (pH 8)/150 mM NaCl. The r*Ov*-GloI was loaded on the column at a flow rate of 60 ml/h, 2 ml fractions were collected, and the enzymic activity towards methylglyoxal was determined.

Blood samples, SDS/PAGE and Western blot analysis

Blood was collected from persons living in a hyperendemic onchocerciasis focus in western Uganda [22]. Microfilarial densities were assessed by skin snip examination. For the first screening for *Ov*-GloI antibodies, sera were selected from patients with high parasite loads of more than 200 microfilariae/mg of skin (range 202–575). Follow-up sera were collected from 11 patients 1 year after treatment with a single dose of the microfilaricidal drug ivermectin (150 μg/kg body weight). As negative controls, two serum pools each containing 10 samples from individuals not infected with *O. volvulus*, but with the filarial parasites *Mansonella streptocerca* and *M. perstans* or with *M. perstans* and the trematode *Schistosoma mansoni*, were used.

SDS/PAGE and Western blotting were performed in accordance with standard techniques [23]. In brief, 5–15 % (w/v) polyacrylamide linear-gradient slab gels were run with r*Ov*-GloI as loading protein at equal concentrations of 4 μg/cm of gel width. Protein was then transferred electrophoretically to nitrocellulose paper with a semi-dry transfer apparatus. Subsequently nitrocellulose was cut into strips, blocked for 1 h with 3 % (w/v) non-fat milk powder in PBS and incubated overnight at 4 °C with patients' sera at dilutions of 1:20 (IgG subclasses) and 1:50 (total IgG). For control, *O. volvulus* total soluble extract was used as antigen. The secondary antibodies (peroxidase-conjugated anti-IgG1, anti-IgG2, anti-IgG3 and anti-IgG4; Calbiochem, La Jolla, CA, U.S.A.) were used at a dilution of 1:1000 and incubated for 1 h at room temperature. Nitrocellulose strips were then developed with 4-chloro-1-naphthol; the enzymic reaction was stopped with doubly distilled water. All incubation steps were separated by washing the nitrocellulose strips with alkaline phosphate buffer.

Quantitative PCR analysis, PCR–ELISA procedure

To determine the expression levels of *Ov*-GloI under different stress conditions, semi-quantitative reverse-transcriptase-mediated PCR (RT–PCR) was performed. For each experiment, RNA from three female *O. volvulus* worms was reverse-transcribed with oligo(dT) primers and the first-strand DNA was analysed with specific *Ov*-GloI primers (forward primer, 5′-TGGGCTCGACTCAGTGCGAATCA-3′; reverse primer, 5′-ATCAGTATGGGGATTAAATATTCGATCC-3′; these represented bases 39–60 and the complementary sequence of bases 445–475 of *Ov*-GloI cDNA respectively). To obtain a biotinylated PCR product that bound easily to a streptavidin-coated microtitre plate, the reverse primer was 5′-biotinylated (Biometra). Amplification was performed for 20 cycles under the following conditions: denaturation at 94 °C for 15 s, annealing at 54 °C for 30 s, extension at 72 °C for 45 s. The number of cycles in the second PCR varied depending on the sequence and the original amount of target mRNA. Analyses of the samples taken from each PCR tube at an interval of five cycles demonstrated that, between 15 and 20 cycles of a second PCR, the exponential phase was measurable over a broad range before the plateau phase.

Detection and analysis of the biotinylated amplified PCR-products were performed with a fluorescein-labelled *Ov*-GloI cDNA fragment (5′-CATGCCGCATATACACTTTTTACCGCTATA-3′) for hybridization in quantitative PCR–ELISA. As an internal control, a primer pair (forward primer, 5′-TTCCGGTATGTGCAAAGCCGGAT-3′; biotinylated reverse primer, 5′-TCTCTGTTCGCCTTTGGATTCAGTGG-3′; these represented bases 65–89 and 351–376 of AI124165.1 cDNA respectively) spanning a 311 bp cDNA fragment of *O. volvulus* actin (AI124165.1) was used in the same tube, in the same reaction. For detection of the internal control, a 274 bp fluorescein-labelled actin fragment was used for hybridization (reverse primer, 5′-GGATGTTCCTCAGGAGCAACTCG-3′, representing bases 310–339). Labelling of the hybridization probes was performed with fluorescein-12-dUTP by using random oligonucleotides as primers (Boehringer Mannheim). The use of the actin gene, which is expressed constitutively, as an internal control permitted a direct measurement to be made of the integrity and quantity of RNA transcripts used in each reverse transcriptase reaction. It also provided a comparable control by which differences in the expression levels, owing to under-

estimation or overestimation of the input amount of the RNA template, could be normalized.

The PCR products were analysed and quantified by ELISA detection. This method is more sensitive than using gel electrophoresis for separation of the PCR products followed by detection of the DNA bands by ethidium bromide or equivalent fluorescent dye. The procedure was performed as described in [24]. Blanks were treated like samples but contained no PCR product. The absorbance readings of the blanks were subtracted from the absorbance readings of the samples; each absorbance reading of *Ov*-GloI was normalized with the respective actin value. Negative controls were obtained by analysing the products of PCR reactions that contained no template cDNA. The cut-off value was defined as the absorbance reading of the negative control plus three times the S.D. The significance of differences between control (unstressed worms) and individual experimental groups was determined by the Kruskal–Wallis test. Statistical significance was defined as $P \leqslant 0.05$.

RESULTS AND DISCUSSION

Characterization of *Ov*-GloI

The complete cDNA of *Ov*-GloI was isolated and contains an open reading frame of 579 bp encoding a protein with a calculated molecular mass of 21930 Da and a theoretical pI of 5.59. Northern blot analysis with complete *Ov*-GloI as probe demonstrated a single transcript of approx. 600 bp that was consistent with the size of the cDNA.

BLAST searches of the deduced amino acid sequence of *Ov*-GloI showed that this clone has similarities to glyoxalase I forms from a wide variety of organisms. Figure 1 shows the multiple alignment of *Ov*-GloI with sequences of a wide spectrum of organisms [*Drosophila melanogaster* (GenBank accession no. AAF59267), human (S63603), potato (Q42891) and *Pseudomonas putida* (P16635)]. The alignment demonstrates that only one gap has been inserted within the structural units (position 122), indicating that the alignment is correct. All the sequences contain the appropriate residues for binding the metal and glutathione, except the *P. putida* sequence, which has a histidine residue in the equivalent position to *Ov*-GloI (Gln-41). It has been shown that the enzyme is still fully active with Zn^{2+} [25]. Although most of the bacterial sequences segregate together, the *P. putida* glyoxalase I is more similar to that of the human enzyme [26]. It is apparent that the N-terminal region of glyoxalase I forms is not well conserved. *Ov*-GloI, for example, has a longer N-terminal stretch of amino acids than the other glyoxalase I forms displayed. Therefore the first 15 residues of *Ov*-GloI could not be aligned to the human enzyme and have not been modelled. The three-dimensional model of *Ov*-GloI was constructed by using the X-ray crystallography data of human glyoxalase I [12,27]. Figure 2 (top panel) shows a structural overlay of human glyoxalase I and *Ov*-GloI. There are no large deviations from the empirical values; the *Ov*-GloI model compares favourably with the structure of human glyoxalase I. The regions encoding the secondary structural elements within the $\beta\alpha\beta\beta\beta$ topology are well conserved. The active site is situated in the dimer interface, with the inhibitor and the essential Zn^{2+} ion interacting with side chains from both subunits (Figure 2, bottom panels). Despite the overall similarity of both binding pockets, there are differences in the hydrophobic substrate-binding pocket. Here, conservative changes in residues (Met-67/Cys-60 and Gly-73/Met-65, subunit I; Phe-182/Leu-174 and Leu-191/Met-183, subunit II) might contribute to size differences of the pocket. Whereas the residues lining the hydrophobic substrate-binding pocket of the human enzyme are hydrophobic, there are two significant differences in the residues of the *Ov*-GloI hydrophobic pocket. In the parasite enzyme we observe that the exchange of Met-179 with Asp-187 and Ile-88 with Lys-96, two charged residues, gives this pocket a more charged character (Figure 3). It could be this variability within the proposed hydrophobic substrate-binding pocket that confers the differential reactivity and substrate/inhibitor specificity observed between *Ov*-GloI and the human enzyme.

Functional expression of *Ov*-GloI in *E. coli*

Heterologous expression of r*Ov*-GloI and purification with *S*-hexylglutathione–agarose were analysed by SDS/PAGE [15%

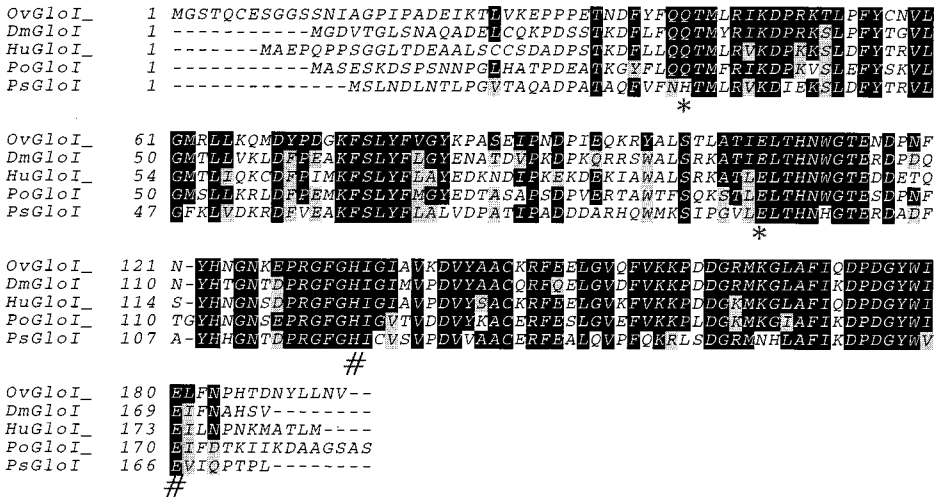

Figure 1 Alignment of *Ov*-GloI with several homologous proteins

The sequences of *Ov*-GloI, *Drosophila melanogaster* glyoxalase I (AAF59267), human glyoxalase I (GenBank accession no. S63603), potato glyoxalase I (Q42891) and *Pseudomonas putida* glyoxalase I (P16635) are shown; gaps indicated by a dash were introduced to optimize the alignment. Residues that are identical or similar with the other glyoxalases are indicated in black when they are all identical and in grey when they are conserved in at least three sequences. The symbols * and # indicate amino acids that are responsible for zinc binding (*, domain A; #, domain B).

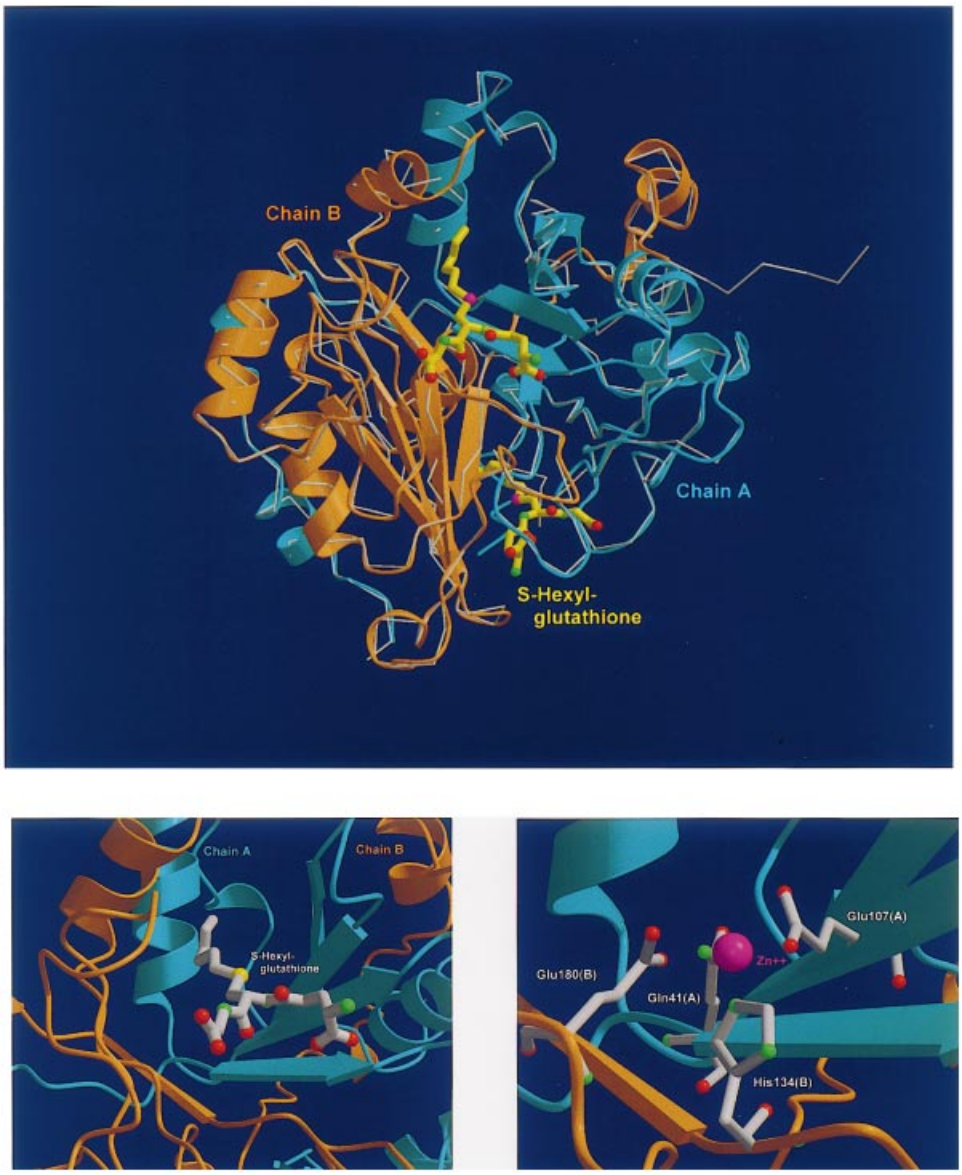

Figure 2 Schematic representations of *Ov*-GloI

Top panel: superposition of the parasitic enzyme *Ov*-GloI with glyoxalase I from the host. Bottom left-hand panel: illustration of the glutathione binding site; a ball-and-stick figure showing the inhibitor *S*-hexylglutathione modelled into the active site with the *S*-hexyl group of the conjugate located in the hydrophobic pocket. Bottom right-hand panel: the Zn^{2+}-binding site is co-ordinated by four conservative protein residues, with each domain contributing two residues to the zinc binding (chain A, Gln-41 and Glu-107; chain B, His-134 and Glu-180).

(w/v) gel] (Figure 4). A 6 mg yield of r*Ov*-GloI was obtained from 1 litre of culture. The purified *Ov*-GloI was stable during purification and storage. Purified r*Ov*-GloI has a molecular mass of approx. 24 kDa, which is in agreement with the value calculated from the cDNA sequence. However, in some preparations two protein bands of approx. 24 and 20 kDa were visible on the SDS/PAGE gel. This might have been due to an additional initiation of the translation at the second methionine residue (Met-42). Truncation of the 5′ end of human glyoxalase I during expression in COS-1 cells has been described, and proteolytic breakdown and initiation at other ATG codons has been discussed [28]. The molecular mass of the enzymically active r*Ov*-GloI was estimated by gel filtration to be 45 kDa. This estimate is close to the sum of two subunits; it was concluded that active r*Ov*-GloI is dimeric. This is consistent with the quaternary structure of glyoxalase I forms from other organisms.

The specific activities of r*Ov*-GloI towards methylglyoxal and phenylglyoxal were 284 ± 32 and 105 ± 10 μmol/min per mg of protein respectively. This is of course much higher than the glyoxalase activity measured in the homogenate of *Onchocerca gutturosa* (0.3311 and 0.1712 μmol/min per mg of protein for methylglyoxal and phenylglyoxal respectively) [29]. The K_m values for methylglyoxal and phenylglyoxal were determined as 340 and 311 μM respectively. In human recombinant glyoxalase I, the K_m for phenylglyoxal is half of that described for methylglyoxal, reflecting the increasing hydrophobicity of the substrate [30]. However, for *Ov*-GloI the K_m values for both substrates were almost equivalent, indicative of the observed

Figure 3 Representation of the hydrophobic substrate-binding pocket

The schematic representation of the backbone has been coloured (white, chain A, green, chain B). The two residues illustrated differ from the human enzyme (Lys-96; Asp-187). The inhibitor *S*-hexylglutathione is indicated in light blue.

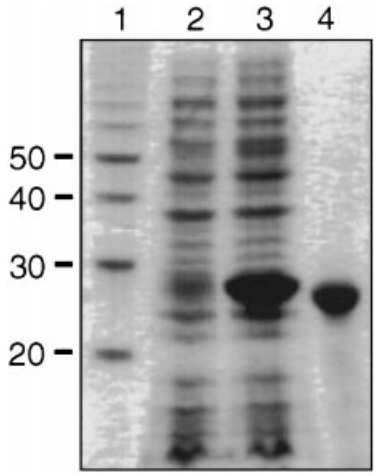

Figure 4 Production and purification of r*Ov*-GloI

Coomassie-stained SDS/PAGE [15% (w/v) gel]. Lane 1, marker proteins (molecular masses indicated in kDa at the left); lane 2, lysate of *E. coli* BL21 containing pJC40-*Ov*-GloI without induction with IPTG; lane 3, lysate of *E. coli* BL21 containing pJC40-*Ov*-GloI, after induction with IPTG; lane 4, affinity-purified r*Ov*-GloI.

differences in the cavity of the hydrophobic substrate-binding site (Figure 3). In comparison with the residues lining the hydrophobic pocket of human glyoxalase I, which are hydrophobic, there is a difference in two residues, namely Asp-187 (Met-179 in human glyoxalase I) and Lys-96 (Ile-88 in human glyoxalase I). The K_m values are approx. 5-fold and 10-fold those described for the recombinant human enzyme with methylglyoxal and phenylglyoxal respectively. However, the magnitude of k_{cat}/K_m for r*Ov*-GloI still reveals the impressive catalytic property of this enzyme (Table 1).

Table 1 Kinetic constant for recombinant *Ov*-GloI

The concentration of free glutathione was maintained at 0.1 mM for all measurements. Values are means ± S.D. for at least triplicate determinations.

Substrate	K_m (μM)	k_{cat} (min^{-1})	$10^7 \times k_{cat}/K_m$ ($M^{-1} \cdot min^{-1}$)
Methylglyoxal	340 ± 53	11900	3.52
Phenylglyoxal	311 ± 10	4900	1.57

The IC_{50} values of several organic compounds with different chemical structures were determined for r*Ov*-GloI. In brief, no inhibition was achieved at concentrations up to 100 μM when using the hydroxynaphthoquinone derivative lapachol and the polyhydroxyflavone fisetin, which are both good inhibitors of human and yeast glyoxalase I (K_i 37.5 and 8.25 μM respectively). Human glyoxalase I has been described as a nitric-oxide-responsive protein [31] and it was postulated that nitrosothiols inhibit glyoxalase I through site-specific mixed disulphide formation at a conserved cysteine residue, converting the enzyme into an inactive isoform. *Ov*-GloI activity remained unchanged after preincubation of the enzyme with *S*-nitrosoglutathione at concentrations up to 100 μM. This failed inhibition probably reflects the fact that, whereas the conserved residue Cys-139 in human glyoxalase I is present in *Ov*-GloI (Cys-146), Cys-61 located in the hydrophobic substrate-binding site in human glyoxalase I is missing from *Ov*-GloI. The IC_{50} values of known inhibitors of human and yeast glyoxalase I were obtained for purpurogallin (15 μM), dichlorophen (48 μM), quercetin (74 μM), oxibendazol (107 μM) and *S*-hexylglutathione (113 μM). Clearly, with the exception of purpurogallin, the compounds tested are weak inhibitors of *Ov*-GloI [32,33].

All parasites need to maintain a high supply of energy for macromolecular synthesis, growth, mechanical activity, differentiation and reproduction. Parasites characteristically exhibit rapid growth or multiplication, which make great demands on energy-generating mechanisms. They also need protection from the immune response of the host, another major energetic cost. All helminths use glucose, which, once absorbed, is either converted into glycogen or metabolized directly via Embden–Meyerhof glycolysis. Thereafter there are several options: helminths are homolactate fermenters, 'mixed acid' fermenters or perform malate dismutation. The main end product of filarial parasites is lactate [34,35]. Therefore, to meet their high energy needs, filarial nematodes have a high rate of anaerobic glycolysis, a high flux of glucotriose and, we propose, a concomitant high rate of formation of methylglyoxal. We therefore suggest that detoxification of the α-oxoaldehydes via the glyoxalase system must be essential for the helminth's survival because 2-oxoaldehydes are cytotoxic at high concentrations.

Glyoxalase I enzymes have been targeted for the development of novel anti-tumour, anti-protozoal and anti-bacterial agents [36–38]; several lead substances are available and will foster further studies with the use of the recombinant protein and with analysis of pro-drugs for potential nematocidal effects.

Serological responses

Because *Ov*-GloI is the first glyoxalase I to be described in detail in a parasitic organism, no information about its natural immunogenicity is available. We therefore performed a Western blot

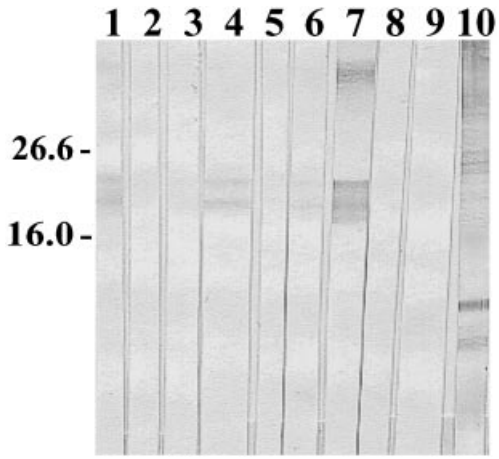

Figure 5 Demonstration of antibodies against r*Ov*-GloI in patient sera

Western blot analysis with r*Ov*-GloI (lane 1–9) or total *O. volvulus* worm extract (lane 10) as antigen and anti-IgG1 as secondary antibody. Sera from patients with high *O. volvulus* microfilarial loads (lanes 1–8 and 10) or from a non-infected individual (lane 9) were tested; specific antibodies against *Ov*-GloI were detected in lanes 1, 4, 6 and 7. The positions of molecular-mass markers are indicated (in kDa) to the left of the Figure.

analysis with r*Ov*-GloI protein as antigen. In total, 42 sera from persons with high microfilarial loads (more than 200 microfilaria/mg of skin) were tested; 5 (12 %) sera gave a positive reaction, showing a characteristic double band at 24 and 21 kDa (Figure 5). IgG isotyping revealed that the antibodies detected belonged to the IgG1 subclass. In addition, follow-up sera from 11 persons 1 year after treatment with the microfilaricidal drug ivermectin were examined. Whereas none of these individuals showed IgG1 antibodies before treatment, 7 (64 %) were positive after treatment, when the microfilarial density had dropped to an average of 3.5 microfilaria/mg of skin (range 0.1–19.6). By using pooled sera from persons not infected with *O. volvulus*, but with the filarial parasites *Mansonella streptocerca* and *M. perstans* and with the trematode *Schistosoma mansoni*, it was shown that the antibody reaction to the *Ov*-GloI protein was specific for *O. volvulus* infection (Figure 5).

These results demonstrate that the *Ov*-GloI protein provokes a humoral immune response in persons infected with *O. volvulus* and that the antibody response is more prominent in persons with low microfilarial counts after treatment with ivermectin. Similar observations have been described for other antigens and it has been shown that immunosuppression due to high microfilarial loads can be restored by treatment with ivermectin [39]. Because the recombinant protein is enzymically active, it is likely that it is correctly folded. Therefore the lack of induction of a humoral immune response in many infected individuals might reflect the high degree of sequence conservation between the parasitic enzyme and that of the host or the intracellular localization. The observed antibody responses to *Ov*-GloI limit the potential of the molecule for immunodiagnosis, although it is relatively specific for *O. volvulus*.

Induction of *Ov*-GloI expression in response to oxidative stress

Exposure to low levels of oxidant stress can enhance the expression of numerous enzymes involved in defence against these oxidants. The induction of these genes is thought to engender resistance to subsequent exposure to high concentrations of oxidants. Similarly, the aquisition of stable resistance to oxidant injury is associated with the increased expression of genes involved in antioxidant defence. We therefore investigated the role of the glyoxalase system in the defence against external or environmental stress (generated outside of the parasite maintained *in vitro*) and endogenous oxidative stress with the prooxidant plumbagin. Quantification analysis via ELISA readings revealed that the levels of mRNA from *Ov*-GloI were increased 3.2-fold ($P \leqslant 0.04$) in response to oxidative stress applied with xanthine/xanthine oxidase and 1.95-fold ($P \leqslant 0.02$) in response to plumbagin. It is probable that this up-regulation is an adaptive response of the parasite to dicarbonyl stress.

The effects of feeding different doses of methylglyoxal to Swiss albino mice were examined by using enzymes involved in the antioxidant function, glutathione contents and lipid peroxidation [40]. The glutathione contents of the liver decreased while there was an increase in lipid peroxidation; it was observed that the specific activity of detoxifying enzymes in the liver decreased significantly. These findings are suggestive of the adverse effect of methylglyoxal on the antioxidant defence system. The concentration of cellular thiols is decreased and this in turn decreases the cysteinyl thiol sites for α-oxoaldehyde storage and the cellular concentration of glutathione, and hence the activity of glyoxalase I *in situ*. In diabetes, oxidative stress and the formation of reactive dicarbonyl compounds are increased [41] and elevated activities of the transcription factors NF-κB (nuclear factor κB) and AP-1 (activator protein 1) have been reported in diabetic rats [42]. Because this effect could be partly prevented by the administration of antioxidants, it was postulated that oxidative stress was involved in the activation of these transcription factors. The promoter activity and the regulation of human glyoxalase I have recently been described [43]. Besides identifying a functionally operative insulin-responsive element and a metal-responsive element, it is suggested that the glyoxalase I gene is regulated by transcription factors AP-1 and NF-κB, whose binding sites have been identified in the promoter region under conditions of oxidative stress.

Recently we have identified a highly stress-responsive *O. volvulus* glutathione S-transferase, *Ov*-GST3, by RT–PCR differential display. The *Ov*-GST3 transcript level increased markedly, by more than 125-fold, in response to oxidative stress applied with xanthine/xanthine oxidase. A role for filarial GSTs in the defence against oxidative stress has been invoked on the basis of several studies; we propose that one important function of the GSTs is to provide a defence against toxic products arising from the host immune-initiated peroxidation of parasite membranes [44,45].

To obtain a clearer picture of the role of the glyoxalases in oxidative/environmental stress in nematodes, we are currently analysing the structural basis of transcriptional regulation and enzymic activities *in situ* of the glyoxalase I gene (C16C10.10) in the model nematode *Caenorhabditis elegans*.

We thank K. Henkle-Dührsen and M. L. Eschbach for kindly supplying us with *O. volvulus* material, and I. Bonow for technical assistance. A portion of this work was conducted by A. S. in partial fulfilment of the requirements for a Ph.D. from the University of Hamburg, Germany. This work was supported by the Deutsche Forschungsgemeinschaft (DFG project Li 791/1-4). P. F. was supported by the scholarship programme 'Infectiology' of the BMBF.

REFERENCES

1 Kale, O. (1998) Onchocerciasis: the burden of disease. Ann. Trop. Med. Parasitol. **92** (Suppl. 1), S101–S115

2 Thornalley, P. J. (1993) The glyoxalase system in health and disease. Mol. Aspects Med. **14**, 287–371

3 Thornalley, P. J. (1998) Glutathione-dependent detoxification of α-oxoaldehydes by the glyoxalase system: involvement in disease mechanisms and antiproliferative activity of glyoxalase I inhibitors. Chem. Biol. Interact. **111–112**, 137–151

4 Dixon, D. P., Cummins, I., Cole, D. J. and Edwards, R. (1998) Glutathione-mediated detoxification systems in plants. Curr. Opin. Plant Biol. **1**, 258–266

5 Milanesa, D. M., Choudhury, M. S., Mallouh, C., Tazaki, H. and Konno, S. (2000) Methylglyoxal-induced apoptosis in human prostate carcinoma: potential modality for prostate cancer treatment. Eur. Urol. **37**, 728–734

6 Westwood, M. E., McLellan, A. C. and Thornalley, P. J. (1994) Receptor-mediated endocytic uptake of methylglyoxal-modified proteins. J. Biol. Chem. **269**, 32293–32298

7 Kalapos, M. P. (1999) On the promine/retine theory of cell division: now and then. Biochim. Biophys. Acta **1426**, 1–16

8 Selkirk, M. E., Smith, V. P., Thomas, G. R. and Gounaris, K. (1998) Resistance of filarial nematode parasites to oxidative stress. Int. J. Parasitol. **28**, 1315–1332

9 Brophy, P. M., Crowley, P. and Barrett, J. (1990) Relative distribution of glutathione transferase, glyoxalase I and glyoxalase II in helminths. Int. J. Parasitol. **20**, 259–261

10 Brophy, P. M., Crowley, P. and Barrett, J. (1990) A novel NADPH/NADH-dependent aldehyde reduction enzyme isolated from the tapeworm *Moniezia expansa*. FEBS Lett. **263**, 305–307

11 Albiez, E. J., Büttner, D. W. and Duke, B. O. L. (1988) Diagnosis and extirpation of nodules in human onchocerciasis. Trop. Med. Parasitol. **39**, 331–346

12 Cameron, A. D., Olin, B., Ridderström, M., Mannervik, B. and Jones, T. A. (1997) Crystal structure of human glyoxalase I – evidence for gene duplication and 3D domain swapping. EMBO J. **16**, 3386–3395

13 Sali, A. and Blundell, T. L. (1993) Comparative protein modelling by satisfaction of spatial restraints. J. Mol. Biol. **234**, 779–815

14 Brooks, B. R., Bruccoleri, R E., Olafson, B. D., States, D. J., Swaminathan, S. and Karplus, M. (1983) CHARMM: a program for macromolecular energy, minimization, and dynamics calculation. J. Comp. Chem. **4**, 187–217

15 Perlman, D. A., Case, D. A., Caldwell, J. W., Ross, W. S., Cheatham III, T. E., DeBold, S., Ferguson, D., Seibel, G. and Kollmann, P. (1995) AMBER, a package of computer programs for applying molecular mechanics, normal mode analysis, molecular dynamics and free energy calculations to simulate the structure and energetic properties of molecules. Comp. Phys. Commun. **91**, 1–41

16 Ponder, J. W. and Richards, F. M. (1987) An efficient Newton-like method for molecular mechanics energy minimization of large molecules. J. Comp. Chem. **8**, 1016–1024

17 Laskowski, R. A., MacArthur, M. W., Moss, D. S. and Thornton, J. M. (1993) PROCHECK: a program to check the stereochemical quality of protein structures. J. Appl. Cryst. **26**, 283–291

18 Meritt, E. A. and Murphy, E. P. M. (1994) Raster 3D Version 2.0, a program for photorealistic molecular graphics. Acta Cryst. **50**, 869–873

19 Clos, J. and Brandau, S. (1994) pJC20 and pJC40: two high-copy-number vectors for T7 RNA polymerase-dependent expression of recombinant genes in *Escherichia coli*. Protein Expr. Purif. **5**, 133–137

20 Ridderström, M. and Mannervik, B. (1996) Optimized heterologous expression of the human zinc enzyme glyoxalase I. Biochem. J. **314**, 463–467

21 Vander Jagt, D. L., Han, L. P. and Lehman, C. H. (1972) Kinetic evaluation of substrate specificity in the glyoxalase-I-catalyzed disproportionation of ketoaldehydes. Biochemistry **11**, 3735–3740

22 Fischer, P., Kipp, W., Bamuhiga, J., Binta-Kahwa, J., Kiefer, A. and Büttner, D. W. (1993) Parasitological and clinical characterization of *Simulium neavei*-transmitted onchocerciasis in western Uganda. Trop. Med. Parasitol. **44**, 311–321

23 Burnette, W. N. (1981) Western blotting: electrophoretic transfer of proteins from sodium dodecyl sulfate-polyacrylamide gels to unmodified nitrocellulose and radiographic detection with antibody and radioiodinated protein A. Anal. Biochem. **112**, 195–203

24 Fischer, P., Liu, X., Lizotte-Waniewski, M., Kamal, I. H., Ramzy, R. M. and Williams, S. A. (1999) Development of a quantitative, competitive polymerase chain reaction–enzyme-linked immunosorbent assay for the detection of *Wuchereria bancrofti* DNA. Parasitol. Res. **85**, 176–183

25 Clugston, S. L. and Honek, J. F. (2000) Identification of sequences encoding the detoxification metalloisomerase glyoxalase I in microbial genomes from several pathogenic organisms. J. Mol. Evol. **50**, 491–495

26 Clugston, S. L., Daub, E. and Honek, J. F. (1998) Identification of glyoxalase I sequences in *Brassica oleracea* and *Sporobolus stapfianus*: evidence for gene duplication events. J. Mol. Evol. **47**, 230–234

27 Ridderström, M., Cameron, A. D., Jones, T. A. and Mannervik, B. (1998) Involvement of an active-site Zn^{2+} ligand in the catalytic mechanism of human glyoxalase I. J. Biol. Chem. **273**, 21623–21628

28 Ranganathan, S., Walsh, E. S., Godwin, A. K. and Tew, K. D. (1993) Cloning and characterisation of human colon glyoxalase I. J. Biol. Chem. **268**, 5661–5667

29 Pemberton, K. D. and Barrett, J. (1989) The detoxification of xenobiotic compounds *by Onchocerca gutturosa* (Nematoda: Filarioidea). J. Parasitol. **19**, 875–878

30 Thornalley, P. J. (1990) The glyoxalase system: new developments towards functional characterization of a metabolic pathway fundamental to biological life. Biochem. J. **269**, 1–11

31 Mitsumoto, A., Kim, K., Oshima, G., Kunimoto, M., Okawa, K., Iwamatsu, A. and Nakagawa, Y. (1999) Glyoxalase I is a novel nitric-oxide-responsive protein. Biochem. J. **344**, 837–844

32 Douglas, K. T., Gohel, D. I., Nadvi, I. N., Quilter, J. and Seddon, A. P. (1985) Partial transition-state inhibitors of glyoxalase I from human erythrocytes, yeast and rat liver. Biochem. Biophys. Acta **829**, 109–118

33 Allen, R. E., Lo, T. W. and Thornalley, P. J. (1993) Inhibitors of glyoxalase I: design, synthesis, inhibitory characteristics and biological evaluation. Biochem. Soc. Trans. **21**, 535–540

34 Wittich, R. M. and Walter, R. D. (1987) *Onchocerca volvulus*: partial glucose catabolism via fumarate and succinate. Exp. Parasitol. **64**, 517–518

35 Powell, J. W., Stables, J. N. and Watt, R. A. (1986) An investigation of the glucose metabolism of *Brugia pahangi* and *Dipetalonema viteae* by nuclear magnetic resonance spectroscopy. Mol. Biochem. Parasitol. **18**, 171–182

36 Hamilton, D. S., Kavarana, M. J., Sharkey, E. M., Eiseman, J. L. and Creighton, D. J. (1999) A new method for rapidly generating inhibitors of glyoxalase I inside tumor cells using S-(N-aryl-N-hydroxycarbamoyl)ethylsulfoxides. J. Med. Chem. **42**, 1823–1827

37 D'Silva, C. and Daunes, S. (2000) Structure-activity study on the in vitro antiprotozoal activity of glutathione derivatives. J. Med. Chem. **43**, 2072–2078

38 Johansson, A., Ridderström, M. and Mannervik, B. (2000) The human glutathione transferase P1-1 specific inhibitor TER117 designed for overcoming cytostatic-drug resistance is also a strong inhibitor of glyoxalase I. Mol. Pharmacol. **57**, 619–624

39 Soboslay, P. T., Dreweck, C. M., Hoffmann, W. H., Lüder, C. G., Heuschkel, C., Görgen, H., Banla, M. and Schulz-Key, H. (1992) Ivermectin-facilitated immunity in onchocerciasis. Reversal of lymphocytopenia, cellular anergy and deficient cytokine production after single treatment. Clin. Exp. Immunol. **89**, 407–413

40 Choudhary, D., Chandra, D. and Kale, R. K. (1997) Influence of methylglyoxal on antioxidant enzymes and oxidative damage. Toxicol. Lett. **93**, 141–152

41 Thornalley, P. J. (1996) Advanced glycation and the development of diabetic complications. Unifying the involvement of glucose, methylglyoxal and oxidative stress. Endocrinol. Metab. **269**, 1–11

42 Nishio, Y., Kashiwagi, A., Taki, H., Shinozaki, K., Maeno, Y., Kojima, H., Maegawa, H., Haneda, M., Hidaka, H., Yasuda, H. et al. (1998) Altered activities of transcription factors and their related gene expression in cardiac tissues of diabetic rats. Diabetes **47**, 1318–1325

43 Ranganathan, S., Ciaccio, P. J., Walsh, E. S. and Tew, K. D. (1999) Genomic sequence of human glyoxalase I: analysis of promoter activity and its regulation. Gene **240**, 149–153

44 Brophy, P. M. and Pritchard, D. I. (1994) Parasitic helminth glutathione S-transferases: an update on their potential as targets for immuno- and chemotherapy. Exp. Parasitol. **79**, 89–96

45 Liebau, E., Eschbach, M. L., Tawe, W., Sommer, A., Fischer, P., Walter, R. D. and Henkle-Dührsen, K. (2000) Identification of a stress responsive *Onchocerca volvulus* glutathione S-transferase (*Ov*-GST3) by RT–PCR differential display. Mol. Biochem. Parasitol. **109**, 101–110

Received 24 July 2000/9 October 2000; accepted 3 November 2000